

Семинар имени профессора Б.С. Ишханова "Фотоядерные исследования. Состояние и перспективы", НИИЯФ МГУ, 26 октября 2023 г.

# Перспективы исследований фотоядерных реакций и развитие квазичастично-фононной модели

*Алексей Павлович Северюхин*

*Лаборатория теоретической физики им. Н.Н.Боголюбова  
Объединенный институт ядерных исследований*

# Источник комптоновского излучения создадут на базе НЦФМ

22 марта 2023

*В Институте ядерной физики им. Г.И. Будкера СО РАН (г. Новосибирск) прошло выездное совещание совета РАН по фундаментальной ядерной физике. Учёные обсудили перспективы развития ядерной фотоники в России и создание источника комптоновского излучения – части многофункционального ускорительного комплекса на базе Национального центра физики и математики (НЦФМ).*



# Квазичастично-фононная модель: Сферические ядра

$$\Psi_\nu(JM) = \left( \sum_i R_i(J\nu) Q_{JM_i}^+ + \sum_{\substack{\lambda_1 i_1 \\ \lambda_2 i_2}} P_{\lambda_2 i_2}^{\lambda_1 i_1}(J\nu) [Q_{\lambda_1 i_1}^+ Q_{\lambda_2 i_2}^+]_{JM} + \sum_{\substack{\lambda_1 i_1 \\ \lambda_2 i_2 \\ \lambda_3 i_3 J'}} T_{\lambda_3 i_3}^{\lambda_1 i_1 \lambda_2 i_2}(J\nu) [[Q_{\lambda_1 i_1}^+ Q_{\lambda_2 i_2}^+]_{J'} Q_{\lambda_3 i_3}^+]_{JM} \right) |0\rangle$$

$\lambda^\pi = 1^-, 2^+, 3^-, \text{ and } 4^+$

$$H = \sum_{\lambda\mu i} \omega_{\lambda i} Q_{\lambda\mu i}^+ Q_{\lambda\mu i} + \frac{1}{2} \sum_{\substack{\lambda_1 \lambda_2 \lambda_3 \\ i_1 i_2 i_3 \\ \mu_1 \mu_2 \mu_3}} \langle \lambda_1 \mu_1 \lambda_2 \mu_2 | \lambda_3 - \mu_3 \rangle \times \\ U_{\lambda_2 i_2}^{\lambda_1 i_1}(\lambda_3 i_3) [Q_{\lambda_1 \mu_1 i_1}^+ Q_{\lambda_2 \mu_2 i_2}^+ Q_{\lambda_3 - \mu_3 i_3} + h.c.].$$

В.Г. Соловьев, Теория атомного ядра. Квазичастицы и фононы.

В.В. Воронов, В.Г. Соловьев, ТМФ 57, 75 (1983)

V.Yu. Ponomarev, Ch. Stoyanov, N. Tsoneva, M. Grinberg, Nucl. Phys. A 635, 470(1998)

# На базе функционала плотности энергии обобщены основные уравнения квазичастично-фононной модели

- Самосогласованное среднее поле
- Гармонические вибрации в пределе малых амплитуд
- Взаимодействие простых и сложных конфигураций

Такие расчеты не требуют введения новых параметров, так как остаточное взаимодействие получено самосогласованным образом с тем же самым функционалом плотности энергии как и среднее поле.

Nguyen Van Giai, Ch. Stoyanov, V. V. Voronov, Phys. Rev. C57,1204 (1998).  
A.P.S., V.V. Voronov, Nguyen Van Giai, Eur. Phys. J. A22, 397 (2004).

# Direct proof of the two-phonon character of the dipole excitations in $^{142}\text{Nd}$ and $^{144}\text{Sm}$ around 3.5 MeV

M. Wilhelm,<sup>1</sup> E. Radermacher,<sup>1</sup> A. Zilges,<sup>2</sup> and P. von Brentano<sup>1</sup>

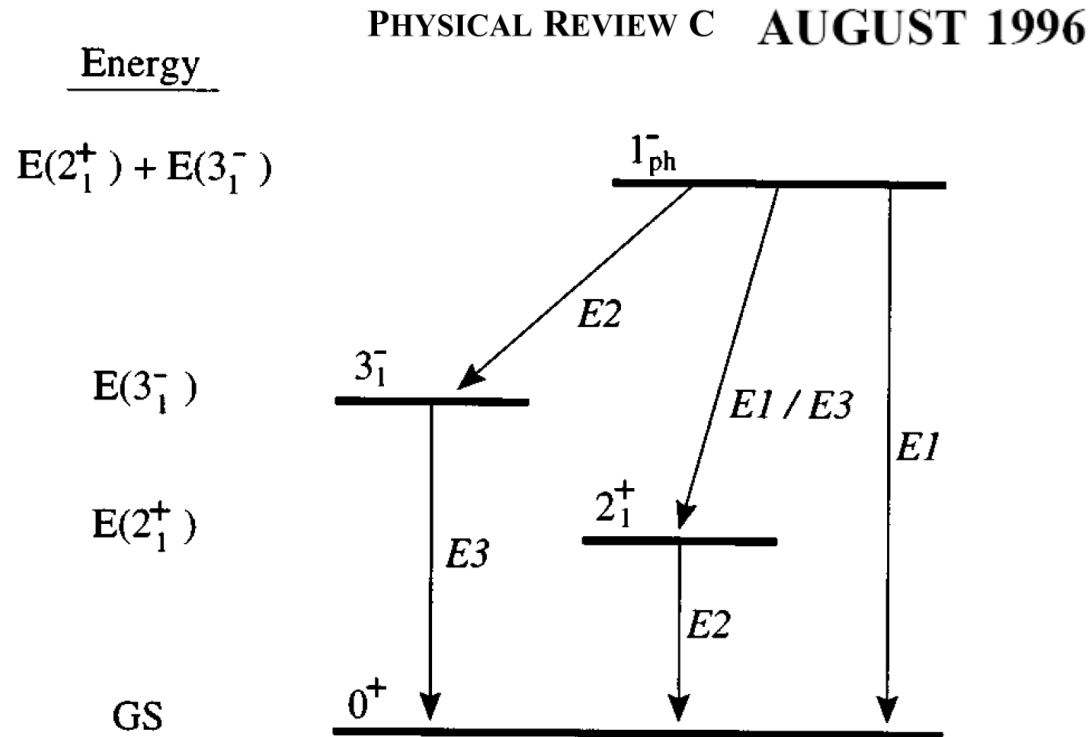
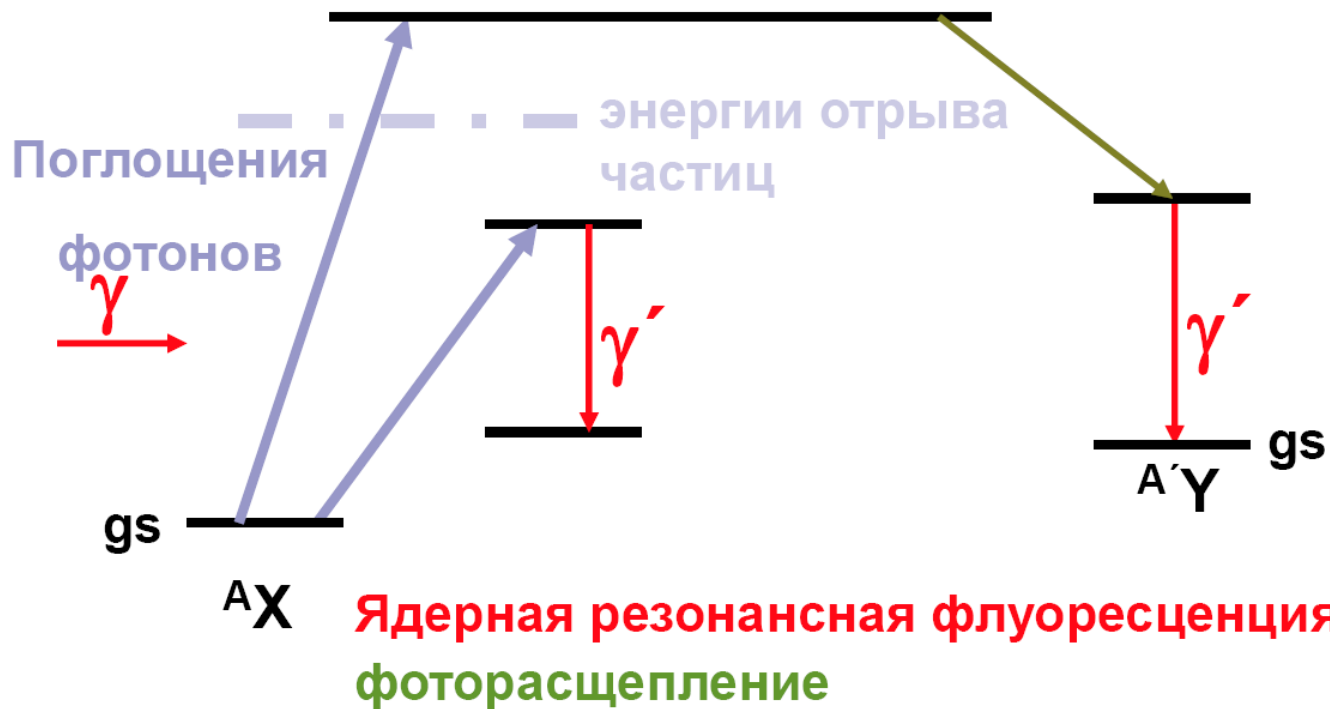


FIG. 1. Decay pattern expected from the  $\gamma$  decay of a two-phonon  $1_{\text{ph}}^-$  state.

Перспективы исследований

$$E_x < 10 \text{ МэВ}$$

# Фотоядерные реакции



Возбуждение дипольных  
альфа-кластерных состояний?  
Пример: состояние  $1^-$   $E_x \sim 7.6$  МэВ  
изотопа кислорода  $^{18}O$

$$S_n \sim 8.0 \text{ МэВ}$$

$$S_\alpha \sim 6.2 \text{ МэВ}$$

Применить к изучению свойств  
двойного гамма-распада?

## NUCLEAR TWO-PHOTON DECAY IN $0^+ \rightarrow 0^+$ TRANSITIONS

J. KRAMP, D. HABS, R. KROTH, M. MUSIC,  
J. SCHIRMER and D. SCHWALM

*Max Planck Institut für Kernphysik and Physikalisches Institut der Universität Heidelberg, FRG*

C. BROUDE

*Weizmann Institute of Science, 76100 Rehovot, Israel*

**Abstract:** The two-photon decay of the first excited  $0^+$  state of  $^{16}\text{O}$  has been measured using the Heidelberg-Darmstadt crystal ball. A branching ratio of  $\Gamma_{\gamma\gamma}/\Gamma_{\text{tot}} = (6.6 \pm 0.5) \cdot 10^{-4}$  was obtained. As in the cases of  $^{40}\text{Ca}$  and  $^{90}\text{Zr}$  previous Experimental matrix elements and properties of the  $0_1^+$  and  $0_2^+$  states in  $^{16}\text{O}$ ,  $^{40}\text{Ca}$  and  $^{90}\text{Zr}$  E1 and M1 transitions of similar strength angular correlation. The ratio of the matrix values  $(-6.2 \pm 1.5)$  or  $(-0.16 \pm 0.04)$ .

An interpretation of  $2\gamma$  matrix elements polarizabilities and magnetic susceptibility decay mode.

Nucleus	$^{16}\text{O}$	$^{40}\text{Ca}$	$^{90}\text{Zr}$
$\Delta E_{12} = E_2 - E_1 [\text{MeV}]$	6.049	3.352	1.761
$T_{1/2} [\text{ns}]$	0.067	2.1	61
$(\Gamma_{\gamma\gamma}/\Gamma_{\text{tot}}) \cdot 10^{-4}$	$6.6 \pm 0.5$	$4.5 \pm 1.0^{\text{d)}$	$1.8 \pm 0.3^{\text{a)}$
$\alpha_{E1}^{12} [10^{-3} \text{fm}^3]$	$16.9 \pm 4.3$	$7.8 \pm 1.9$	$20.1 \pm 10.9$
$\chi^{12} [10^{-3} \text{fm}^3]$	$-2.7 \pm 0.7$ $(-16.9 \pm 4.3)$	$-18.3 \pm 4.5$	$-10.4 \pm 5.7$
$\alpha_{E2}^{12} [\text{fm}^5]$	$\leq 120$	$\leq 670$	$\leq 4000$
$\langle 0_1^+   \bar{r}^2   0_2^+ \rangle [ \text{fm}^2 ]$	$3.55 \pm 0.21^{\text{b)}$	$2.6 \pm 0.1^{\text{c)}$	$1.71 \pm 0.06^{\text{d)}$
$\alpha_{E1}^{11} [10^{-3} \text{fm}^3]$	$585^{\text{e)}$	$2230^{\text{e)}$	$6330^{\text{e)}$
$\chi_{\text{P}}^{11} [10^{-3} \text{fm}^3]$	$1.78^{\text{f)}$	$5.65^{\text{f)}$	$14.5^{\text{f)}$
$\bar{E}_{E1} - E_1 [\text{MeV}]$	$24^{\text{e)}$	$20.2^{\text{e)}$	$16.7^{\text{g)}$
$\bar{E}_{M1} - E_1 [\text{MeV}]$	$17^{\text{h)}$	$10^{\text{h)}$	$9^{\text{j)}$



# Observation of the competitive double-gamma nuclear decay

C. Walz<sup>1</sup>, H. Scheit<sup>1</sup>, N. Pietralla<sup>1</sup>, T. Aumann<sup>1</sup>, R. Lefol<sup>1,2</sup> & V. Yu. Ponomarev<sup>1</sup>

The double-gamma ( $\gamma\gamma$ )-decay of a quantum system in an excited state is a fundamental second-order process of quantum electrodynamics. In contrast to the well-known single-gamma ( $\gamma$ )-decay, the  $\gamma\gamma$ -decay is characterized by the simultaneous emission of two  $\gamma$  quanta, each with a continuous energy spectrum. In nuclear physics, this exotic decay mode has only been observed for transitions between states with spin-parity quantum numbers  $J^\pi = 0^+$  (refs 1–3). Single-gamma decays—the main experimental obstacle to observing the  $\gamma\gamma$ -decay—are strictly forbidden for these  $0^+ \rightarrow 0^+$  transitions. Here we report the observation of the  $\gamma\gamma$ -decay of an excited nuclear state ( $J^\pi = 11/2^-$ ) that is directly competing with an allowed  $\gamma$ -decay (to ground state  $J^\pi = 3/2^+$ ). The branching ratio of the competitive  $\gamma\gamma$ -decay of the  $11/2^-$  isomer of  $^{137}\text{Ba}$  to the ground state relative to its single  $\gamma$ -decay was determined to be  $(2.05 \pm 0.37) \times 10^{-6}$ . From the measured angular correlation and the shape of the energy spectra of the individual  $\gamma$ -rays, the contributing combinations of multiplicities of the  $\gamma$  radiation were determined. Transition matrix elements calculated using the quasiparticle-phonon model reproduce our measurements well. The  $\gamma\gamma$ -decay rate gives access to so far unexplored important nuclear structure information, such as the generalized (off-diagonal) nuclear electric polarizabilities and magnetic susceptibilities<sup>3</sup>.

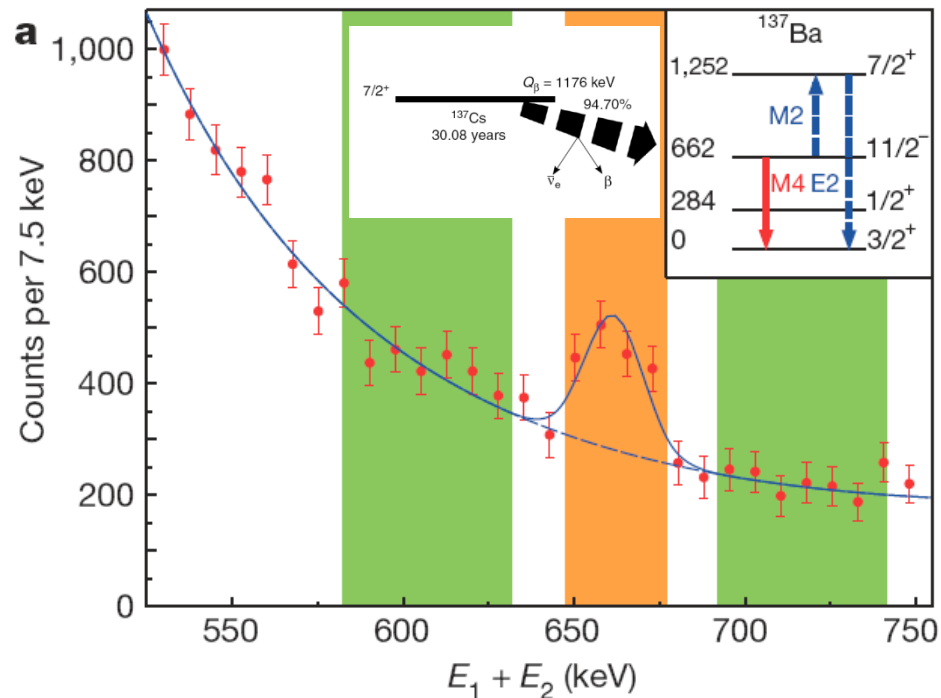


**Figure 2 | Energy-sum spectrum and energy-gated time spectra of the 72°-group.** **a**, Energy-sum spectrum  $E_1 + E_2$  after subtraction of the random coincidences (requiring the energy condition  $|E_1 - E_2| < 300$  keV). The spectrum is fitted with a superposition of a Gaussian and an exponential function to describe the peak and the background, respectively. The orange ( $647 \text{ keV} < E_1 + E_2 < 677 \text{ keV}$ ) and green areas ( $582 \text{ keV} < E_1 + E_2 < 632 \text{ keV}$  and  $692 \text{ keV} < E_1 + E_2 < 742 \text{ keV}$ ) represent the energy conditions employed

ARTICLE



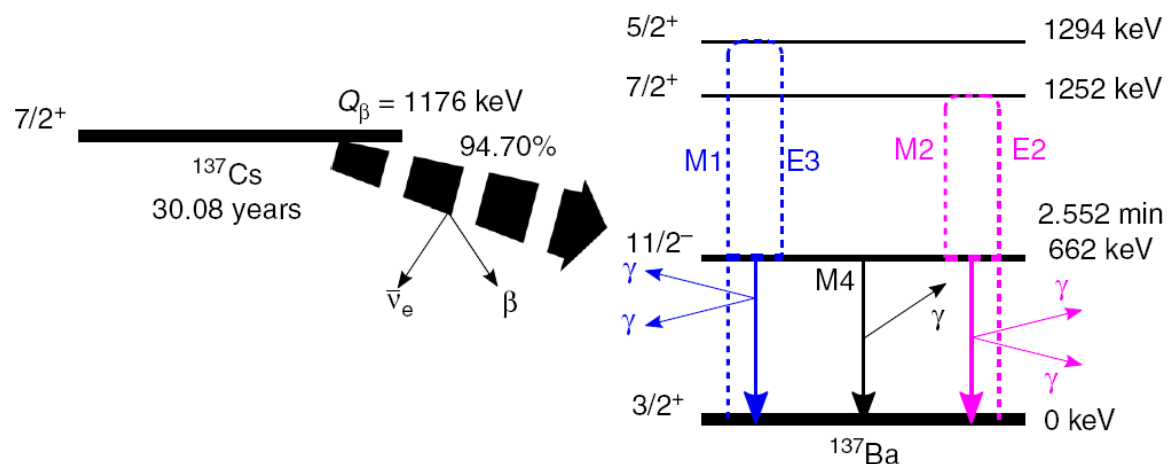
<https://doi.org/10.1038/s41467-020-16787-4>

OPEN

# Electromagnetic character of the competitive $\gamma\gamma/\gamma$ -decay from $^{137m}\text{Ba}$

P.-A. Söderström<sup>1</sup>, L. Capponi<sup>1</sup>, E. Açıksöz<sup>1</sup>, T. Otsuka<sup>2,3,4</sup>, N. Tsoneva<sup>1</sup>, Y. Tsunoda<sup>2</sup>, D. L. Balabanski<sup>1</sup>, N. Pietralla<sup>5</sup>, G. L. Guardo<sup>1,6</sup>, D. Lattuada<sup>1,6,7</sup>, H. Lenske<sup>8</sup>, C. Matei<sup>1</sup>, D. Nichita<sup>1,9</sup>, A. Pappalardo<sup>1</sup> & T. Petrusse<sup>1,9</sup>

Second-order processes in physics is a research topic focusing attention from several fields worldwide including, for example, non-linear quantum electrodynamics with high-power lasers, neutrinoless double- $\beta$  decay, and stimulated atomic two-photon transitions. For the electromagnetic nuclear interaction, the observation of the competitive double- $\gamma$  decay from  $^{137m}\text{Ba}$  has opened up the nuclear structure field for detailed processes through the manifestation of off-diagonal nuclear this observation with an  $8.7\sigma$  significance, and an improvement versus single-photon branching ratio as  $2.62 \times 10^{-6}(30)$ . Our conclusions from the original experiment, where the decay  $\nu$  by a quadrupole-quadrupole component. Here, we find a : energy distribution consistent with a dominating octupole-dip quadrupole-quadrupole component in the decay, hindered d nuclear structure. The implied strongly hindered double-phot the possibility of the double-photon branching as a feasible t on off-diagonal polarisability in nuclei where this hindrance



# Двойной гамма-распад квадрупольного состояния

Using  $\hbar = c = 1$ , the  $\gamma$ -decay width of the  $2_1^+$  state of and even-even nuclei is related to its reduced electric quadrupole transition strength,  $B(E2; 2_1^+ \rightarrow 0_{gs}^+)$ , via

$$\Gamma_\gamma = \frac{4\pi}{75} \left( E_{2_1^+} \right)^5 B(E2; 2_1^+ \rightarrow 0_{gs}^+).$$

To describe the  $\gamma\gamma$ -decay between the  $2_1^+$  and  $0_{gs}^+$  states, we use a formalism that explicitly relates the electromagnetic interaction up to second order in the electromagnetic operators and two-quantum processes in atomic nuclei. Thus, the  $\gamma\gamma$ -decay width can be estimated as

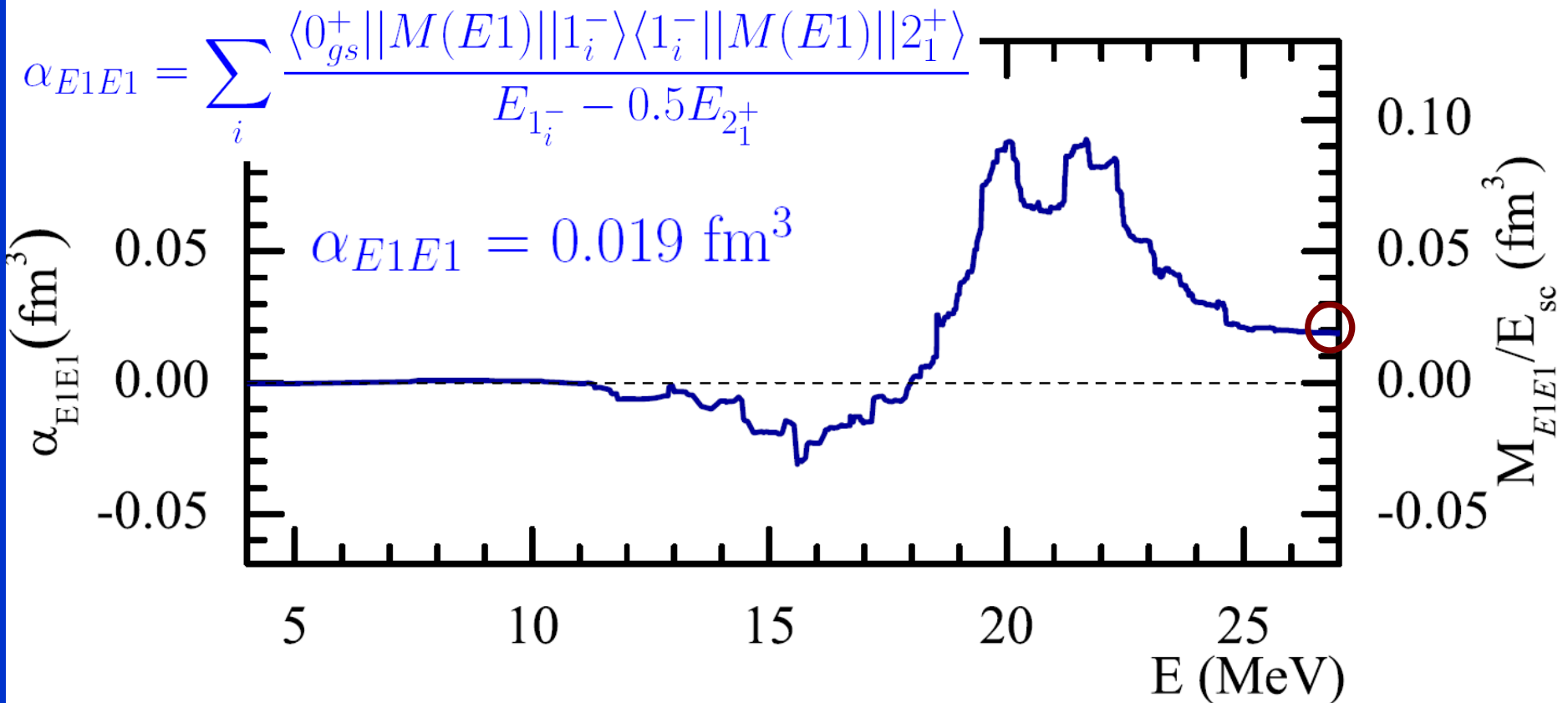
$$\Gamma_{\gamma\gamma'} = \frac{64\pi}{42525} \left( E_{2_1^+} \right)^7 (\alpha_{E1E1})^2 (1 + \delta),$$

with

$$\alpha_{E1E1} = \sum_i \frac{\langle 0_{gs}^+ || M(E1) || 1_i^- \rangle \langle 1_i^- || M(E1) || 2_1^+ \rangle}{E_{1_i^-} - 0.5 E_{2_1^+}},$$

$$\delta = \left( \frac{\alpha_{M1M1}}{\alpha_{E1E1}} \right)^2 + \frac{3}{11} 10^{-4} \left( \frac{\alpha_{E2E2}}{\alpha_{E1E1}} \right)^2 (E_{2_1^+})^4 + \dots$$

The  $\gamma\gamma$ -decay width is dominated by the  $E1E1$  contribution, i.e.,  $\delta \ll 1$ . The case of  $^{48}\text{Ca}$ :  $\delta(M1) = 1.7 \times 10^{-3}$  and  $\delta(E2) = 1.9 \times 10^{-7}$ .



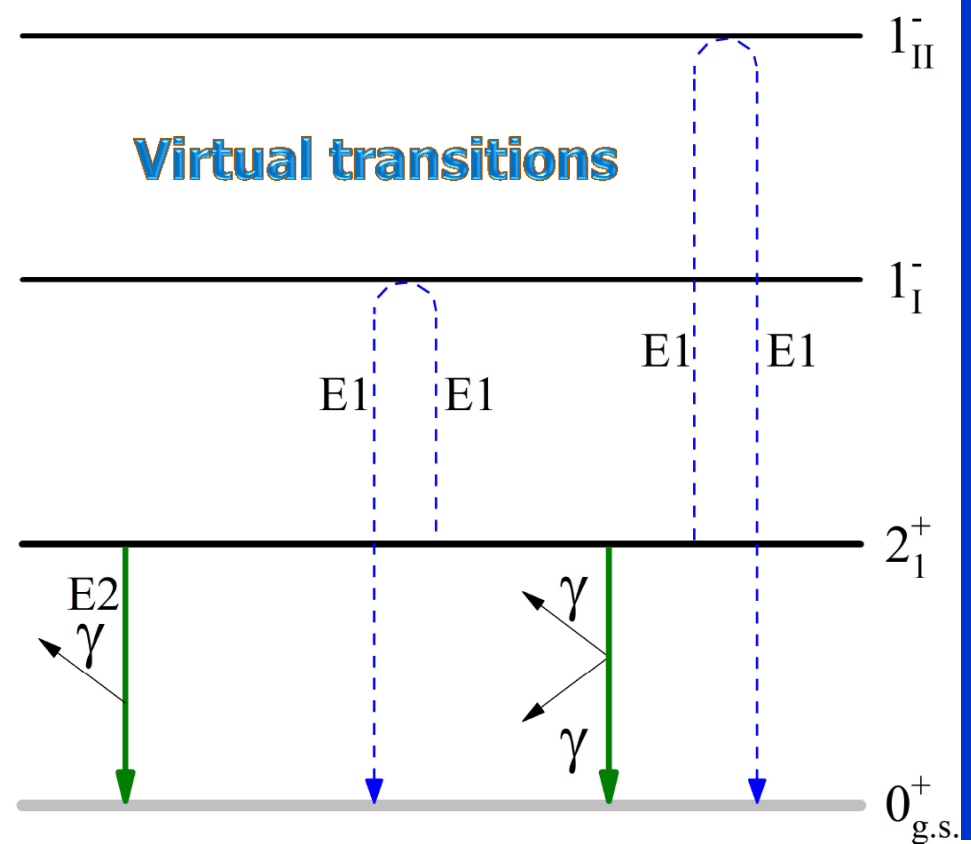
the  $2_1^+$  state of  $^{48}\text{Ca}$ :

**Theory**

$E_x = 3.19 \text{ MeV}$   $B(E2) = 1.3 \text{ W.u.}$   $\Gamma_\gamma = 3.5 \times 10^{-3} \text{ eV}$

$\Gamma_{\gamma\gamma} = 1.0 \times 10^{-10} \text{ eV}$   $\frac{\Gamma_{\gamma\gamma}}{\Gamma_\gamma} = 3 \times 10^{-8}$

# Двойной гамма-распад квадрупольного состояния



We construct a two-state mixing scheme by considering the  $GDR$  state, the coupled  $GDR \otimes 2_1^+$  state, and the interaction  $V$  between them. The relative phases of amplitudes are opposite in the perturbed states I and II, i.e.,

$$|1_I^-\rangle = \alpha|GDR\rangle + \beta|GDR \otimes 2_1^+\rangle,$$

$$|1_{II}^-\rangle = -\beta|GDR\rangle + \alpha|GDR \otimes 2_1^+\rangle.$$

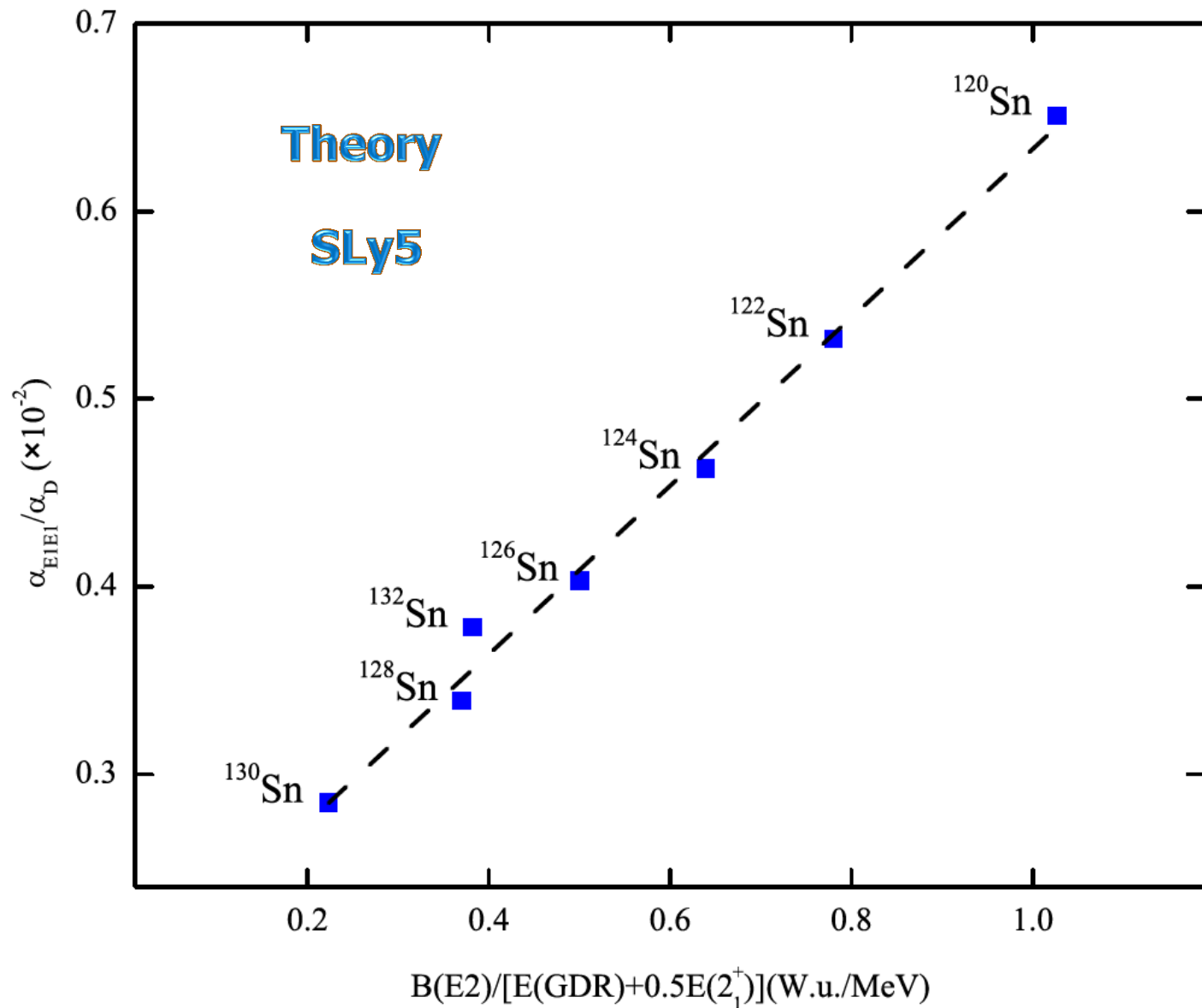
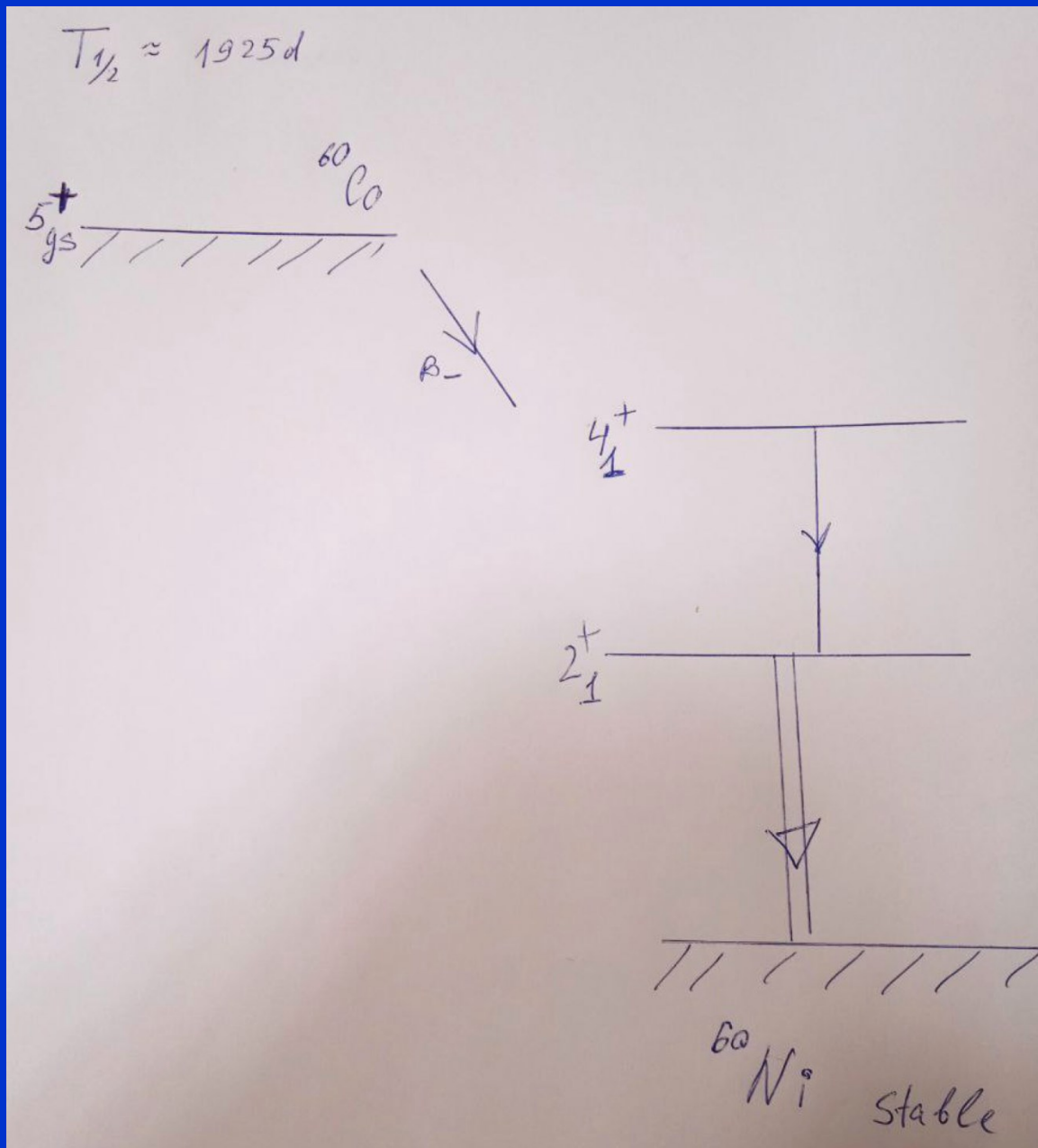


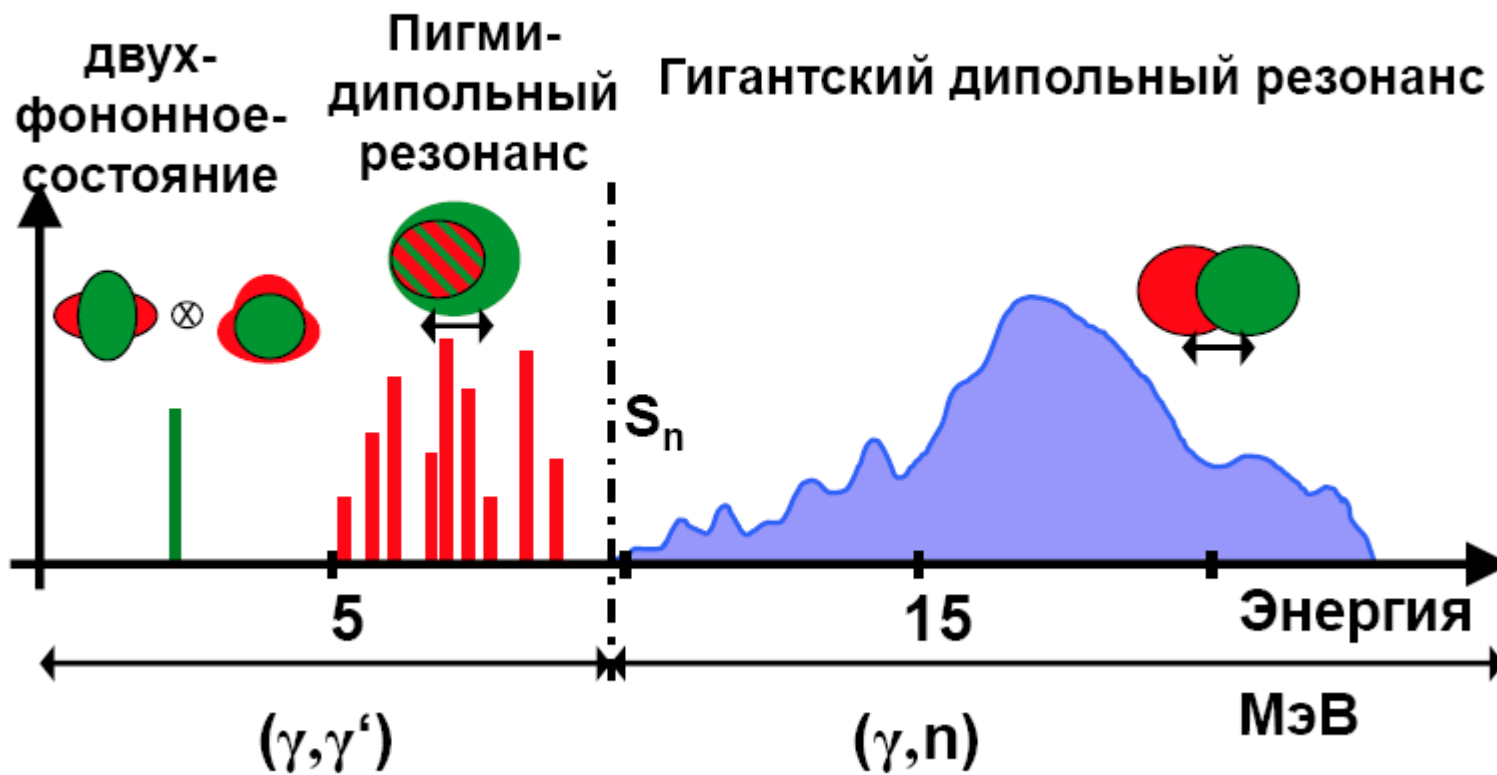
**Figure 1.** The ratio between polarizabilities  $\alpha_{E1E1}$  and  $\alpha_D$  as a function of  $B(E2; 2_1^+ \rightarrow 0_{gs}^+)$  value with respect to the energy centroid of the GDR ( $E(GDR)$ ) and the  $2_1^+$  energy ( $E(2_1^+)$ ). The  $\alpha_{E1E1}/\alpha_D$  evolution of neutron-rich tin isotopes (squares) is calculated taking into account the phonon-phonon coupling based on the SLy5 EDF. The dashed line corresponds to the linear fit predicted Eq. (6).

# предложение эксперимента в рамках проекта ИКИ?





# Распределение силы E1-переходов



# Учет пикми резонанса в расчете r-процесса

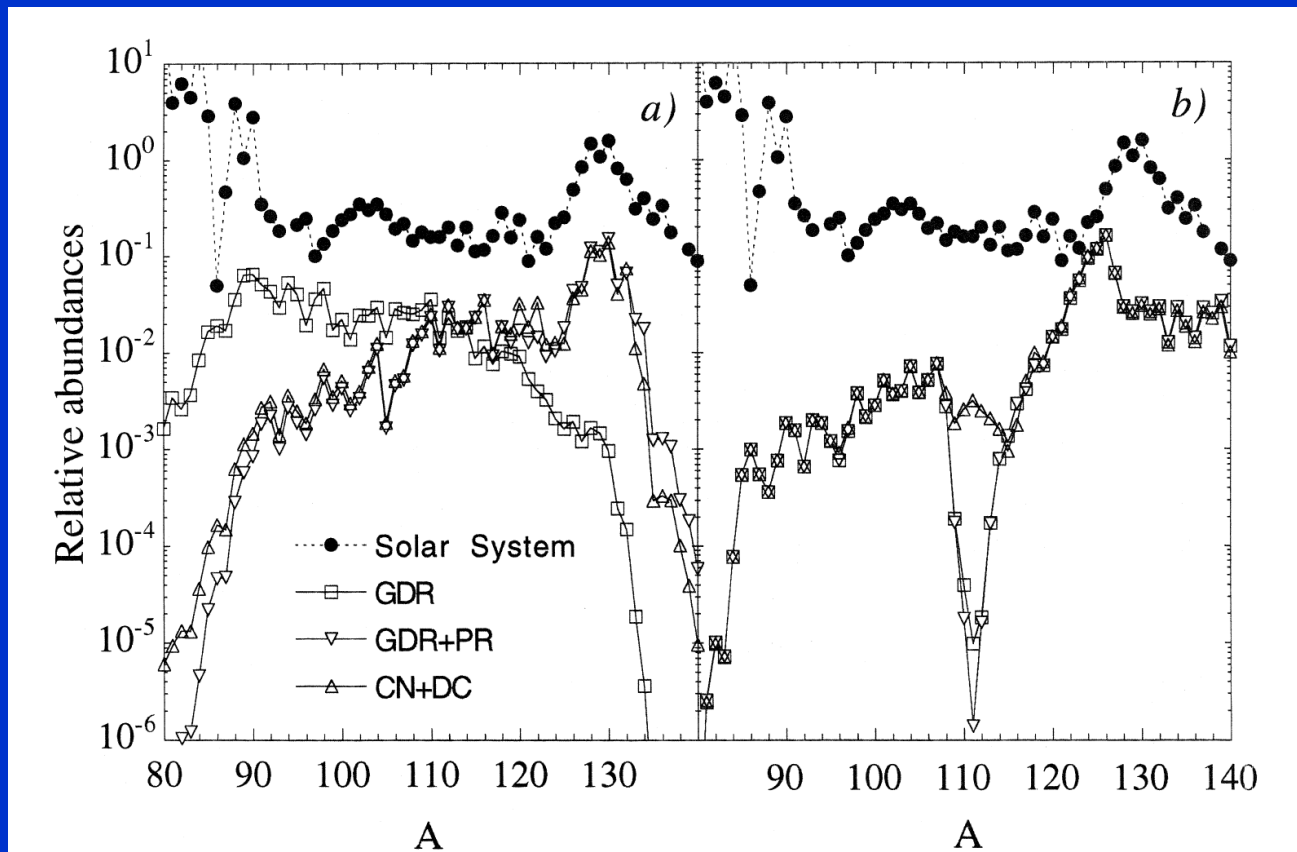
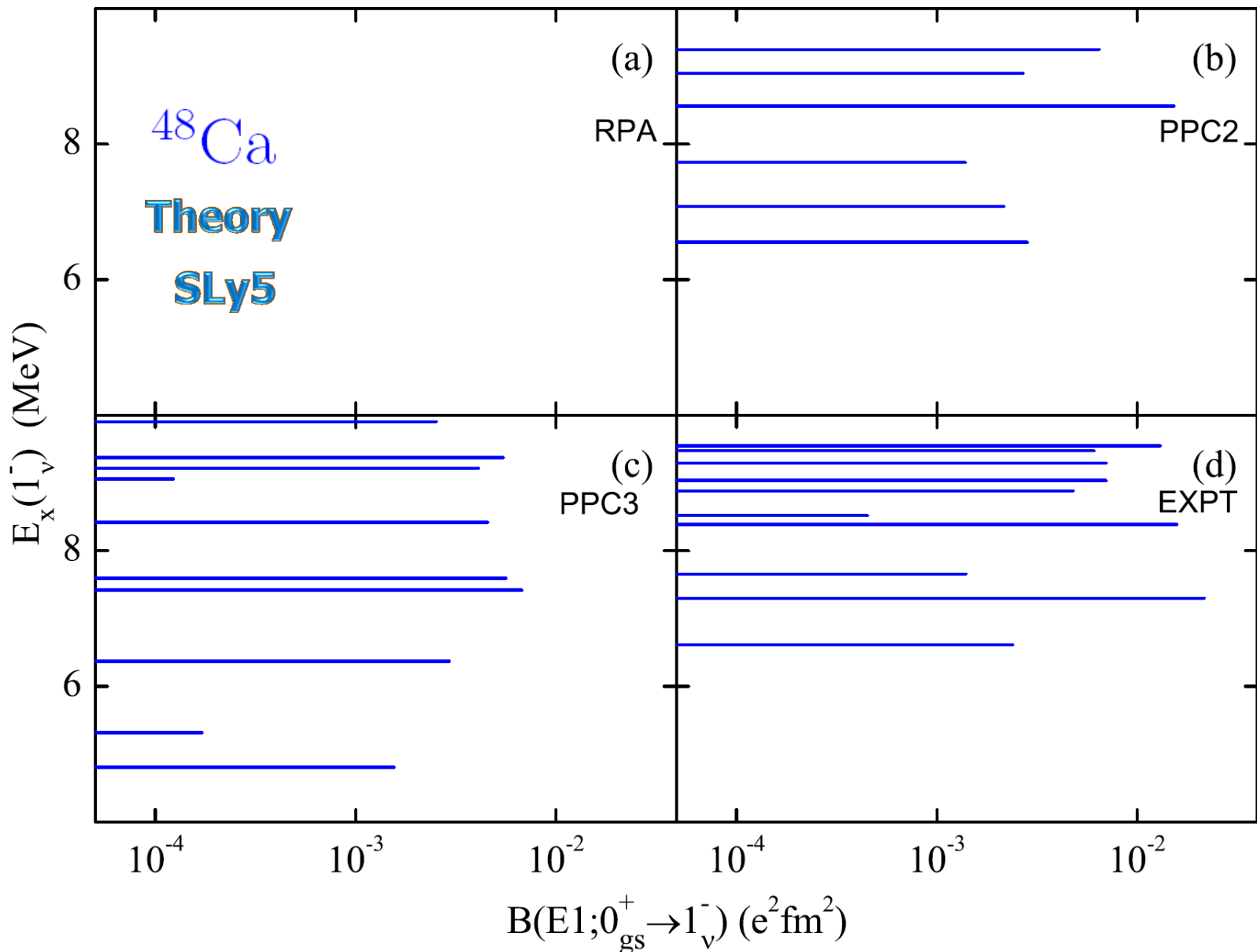


Fig. 6. a) r-abundance distributions for  $T = 10^9$  K,  $N_n = 10^{20} \text{ cm}^{-3}$  and  $\tau_{\text{irr}} = 2.4$  s with 3 different estimates of the neutron capture rates: the standard GDR component, the GDR + PR strength and the damped statistical (CN) plus DC contribution. The top curve corresponds to the solar r-abundances arbitrarily normalized. b) same as a) for  $T = 1.5 \times 10^9$  K,  $N_n = 10^{28} \text{ cm}^{-3}$  and  $\tau_{\text{irr}} = 0.3$  s.



# Перспективы исследований

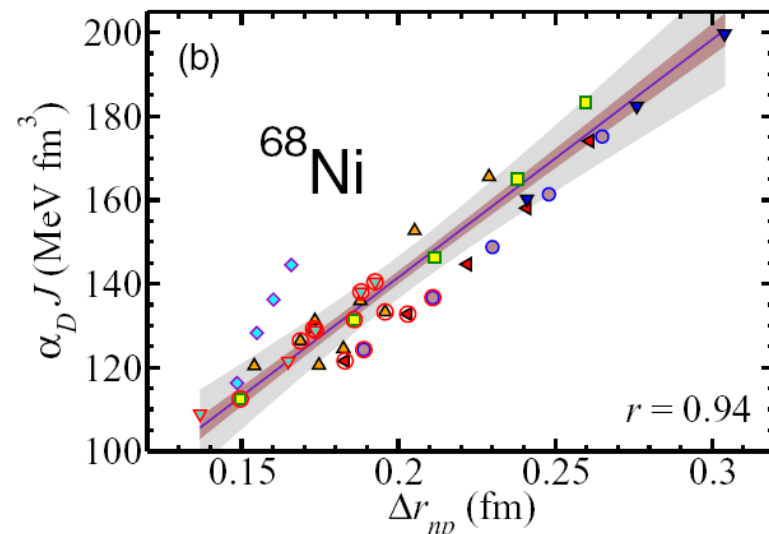
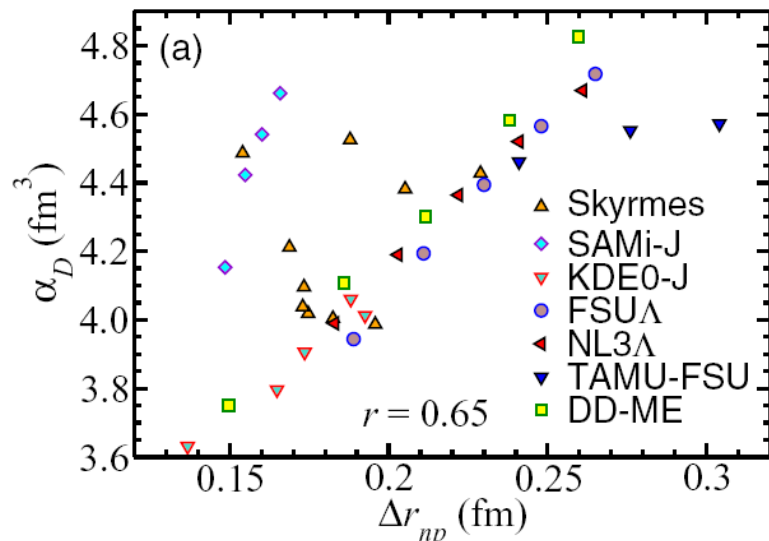
$$10 \text{ МэВ} < E_x < 60 \text{ МэВ}$$

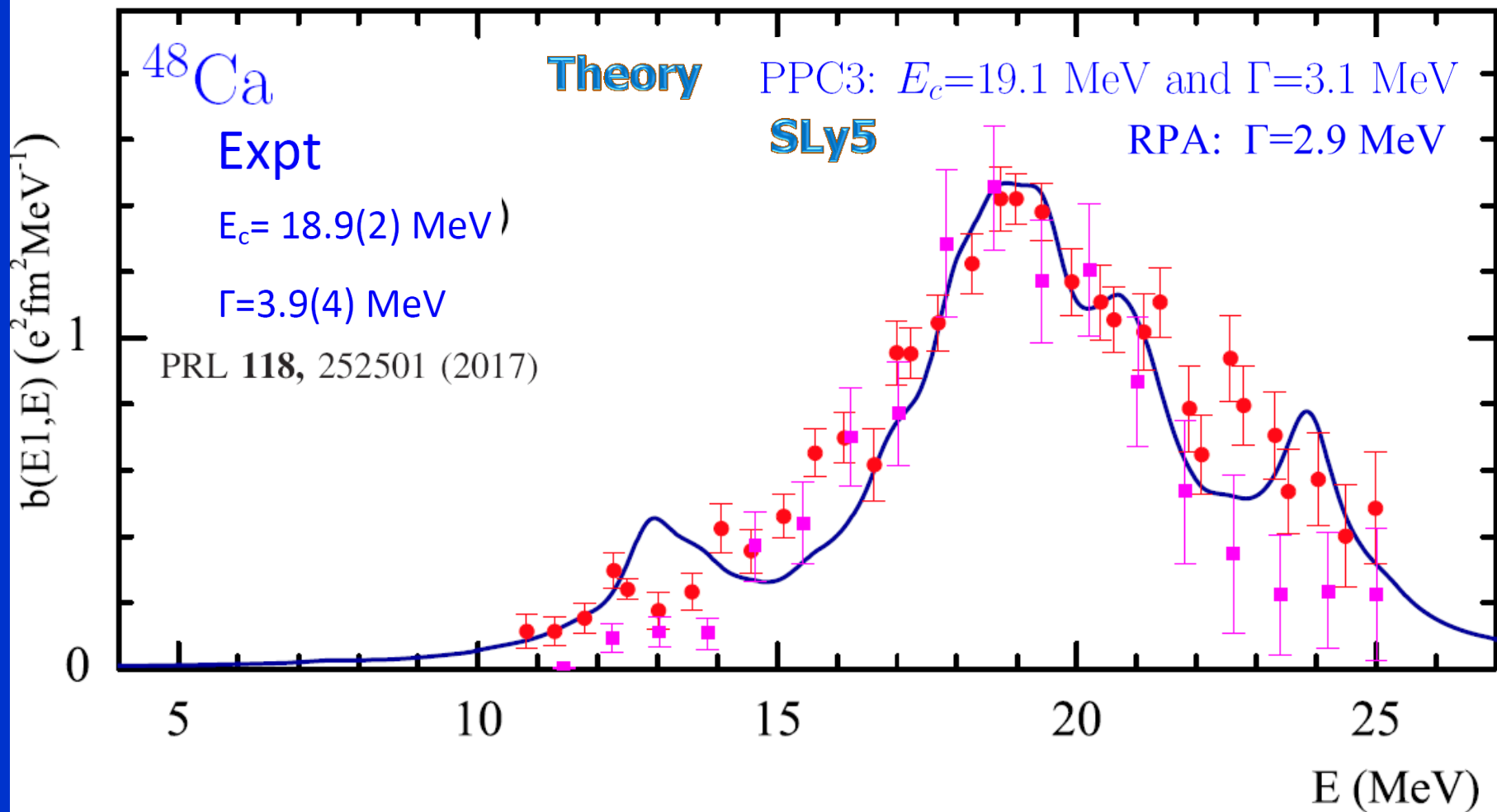
- Электрическая дипольная поляризуемость ядра
- Тонкая структура гигантского резонанса

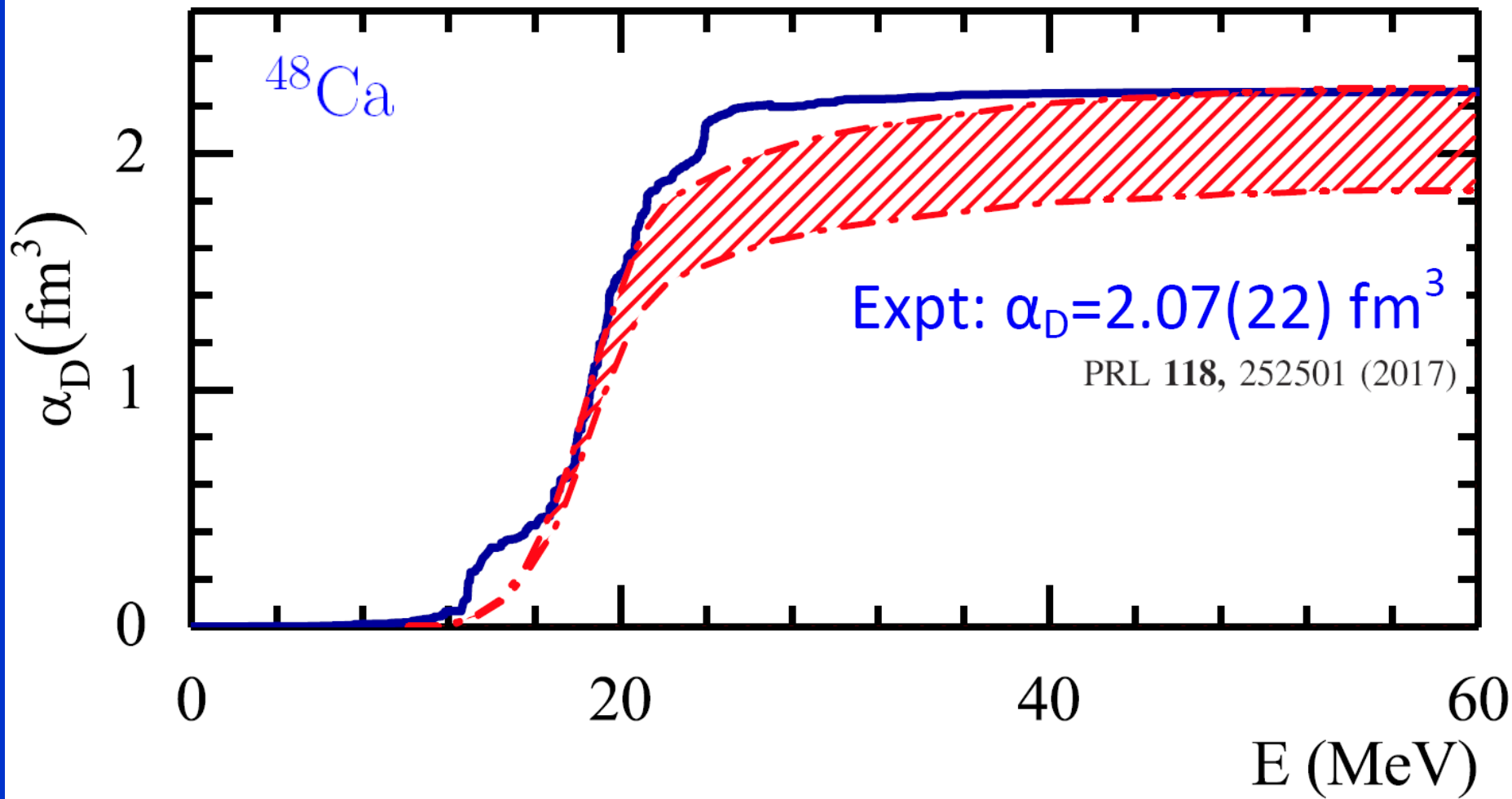
The electric dipole polarizability,

$$\alpha_D = \frac{8\pi}{9} \sum_i \frac{\langle 0_{gs}^+ || M(E1) || 1_i^- \rangle \langle 1_i^- || M(E1) || 0_{gs}^+ \rangle}{E_{1_i^-}},$$

have played an important role, in particular, its value has strong implications in constraining the symmetry energy  $J$  as well as its density dependence and slope parameter  $L$ . The symmetry energy also plays an important role in nuclei, where it contributes to the formation of neutron skins in the presence of a neutron excess.







$$\alpha_D = \frac{8\pi}{9} \sum_i \frac{\langle 0_{gs}^+ || M(E1) || 1_i^- \rangle \langle 1_i^- || M(E1) || 0_{gs}^+ \rangle}{E_{1_i^-}}$$

# Идентификация природы дипольных возбуждений

В рамках проекта ИКИ появляется  
уникальная возможность  
экспериментально исследовать  
 $E_x > 20$  МэВ

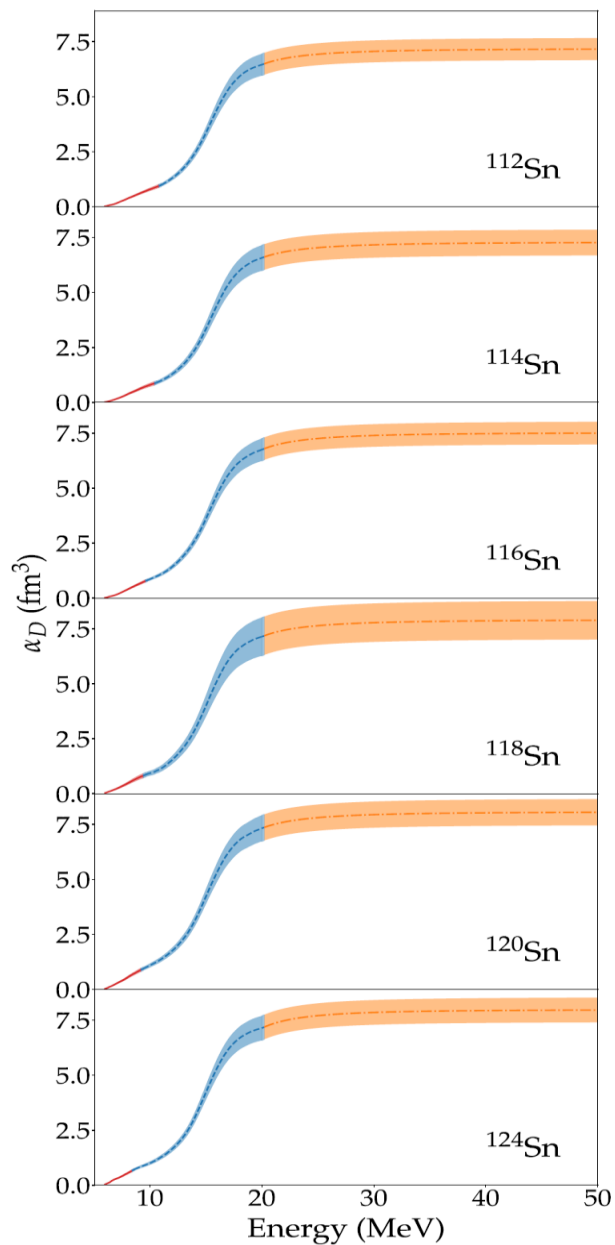


FIG. 20. Running sums of the dipole polarizability deduced from the present ( $p, p'$ ) data. Red: Contribution from 6 MeV to  $S_n$ . Blue: Contribution from  $S_n$  to 20 MeV. Orange: Contribution above 20 MeV from OPM calculations; see text for details.



# Тонкая структура гигантского дипольного резонанса

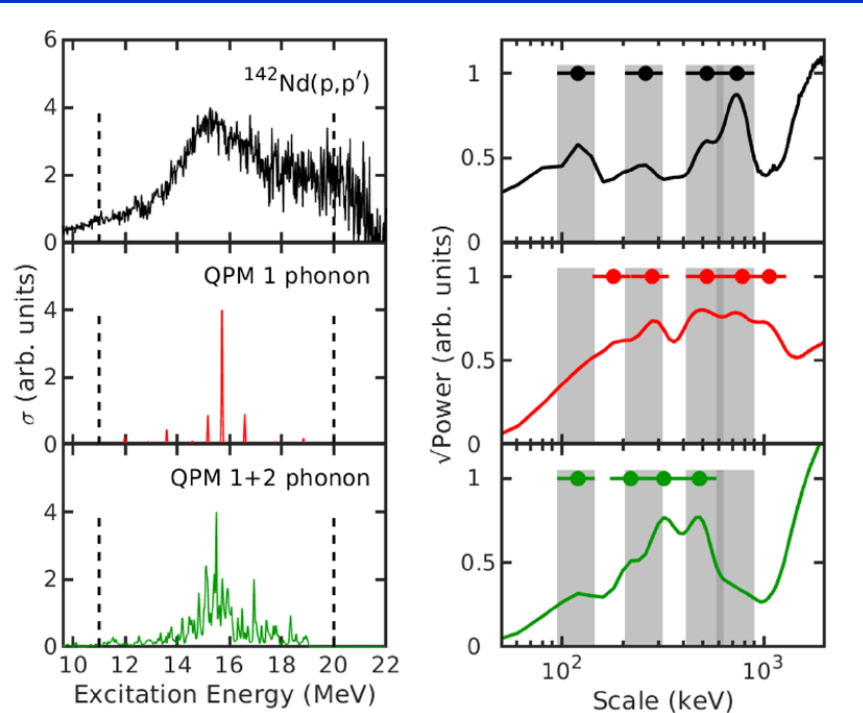


FIG. 10. Left column: Equivalent photoabsorption spectrum for  $^{142}\text{Nd}$  (top) in comparison with the QPM 1 phonon (middle) and QPM 1 + 2 phonon (bottom) model predictions. The vertical dashed lines indicate the excitation-energy region from 11 to 20 MeV over which the wavelet coefficients were summed in order to determine the corresponding power spectra. Right column: Corresponding power spectra where the positions of the scales are indicated by filled circles together with error bars for the width. The experimental scales are also indicated by vertical grey bars in each panel to allow direct visual comparison with the theoretical predictions.

В рамках проекта ИКИ  
появляется возможность  
получить детальную  
информацию о сечениях  
фотоядерных реакций

TABLE I. Energy scales extracted for  $^{142}\text{Nd}$ .

Dataset	Scales (keV)				
Expt.	120	260	520	740	
QPM 1 phonon		180 280	520	780	1060
QPM 1+2 phonon	120	220 320	480		

СПАСИБО ЗА ВНИМАНИЕ